Contrasting garnet parageneses in a composite Grenvillian granitoid pluton, Newfoundland

J. VICTOR OWEN AND ROBERT A. MARR*

Department of Geology, Saint Mary's University, Halifax, Nova Scotia, Canada B3H 3C3

Abstract

Almandine- and grossular-rich garnet occurs as both a coronitic and non-coronitic phase in ferruginous, Grenvillian (*c.* 1050 Ma) granitoid rocks of the composite Potato Hill pluton of the Long Range Inlier, Newfoundland. The country rock includes garnetiferous gneiss, but garnets in the pluton are compositionally distinct (higher Ca and Mn, lower Mg), so none are interpreted as xenocrysts from the Long Range gneiss complex.

Coronal garnet, quartz and hornblende separate primary pyroxene, ilmenite and hornblende from feldspar in two-pyroxene charnockite. Balanced mass-transfer reactions based on microprobe data and modes for the pyroxene-centred corona structures suggest that corona sites gained Fe and lost Na. The flux of Fe apparently controlled corona growth in the charnockite. The corona structures are attributed to subsolidus cooling of the pluton rather than to a metamorphic overprint because the coronas are obliterated in high strain zones cutting the charnockite. Temperature of formation is constrained at *c.* 775–630 °C by two-pyroxene and garnet–hornblende thermometry. Compositionally-similar coronas in rare, Fe-rich enderbite of the Long Range gneiss complex probably formed during cooling after early, high-grade metamorphism or following the regional emplacement of the Grenvillian plutons.

Non-coronitic garnets occur in equigranular and megacrystic hornblende–biotite granite. Garnets in the equigranular granite are large, well-formed, and in some instances are associated with compositional layering of probable igneous origin. These garnets are enriched in grossular ($X_{Ca} = 0.28$), and are therefore interpreted as phenocrysts crystallized at high pressure (>9 kbar?). They would nevertheless have been stabilized to lower pressures by their moderate spessartine content ($X_{Mn} = 0.13$).

Garnets in foliated megacrystic granite form tiny crystals depleted in Fe and Mg, and enriched in Mn and Ca, and in these respects are similar to garnet in deformed charnockite. These garnets are therefore interpreted to have formed (or re-equilibrated) during the late Grenvillian deformation. Garnet is absent in relatively magnesian Grenvillian granites (bulk $X_{Fe^{2+}} = 0.50$–0.85) elsewhere in the inlier. The restriction of garnet to the Potato Hill pluton (bulk $X_{Fe^{2+}} = 0.88$–0.94) therefore testifies to bulk compositional controls on the formation of both magmatic and subsolidus garnet in this intrusion.

KEYWORDS: garnet, corona structure, Grenvillian granites, Newfoundland, Canada.

Introduction

GARNET is a characteristic mineral of peraluminous (e.g. S-type) granites, but is relatively rare in metaluminous, calc-alkaline plutons. Considerable controversy has surrounded the interpretation of garnet in granitoid rocks. Although in some cases it appears to be magmatic in origin, in other instances garnet may be interpreted as a refractory xenocrystic phase (i.e. restite) derived from metamorphic source rocks (e.g. Stone, 1988) or as having a metasomatic origin (e.g. Kontak and Corey, 1988). Magmatic garnets have been interpreted as being indicative of (1) crystallization at elevated pressures ($P \geq 7$ kbar; Green, 1977), or (2) crystallization (possibly at reduced f_{O_2} or f_{H_2O}) at relatively low pressures, at least in evolved peraluminous magmas (Allan and Clarke, 1981; Cawthorne and Brown, 1976, 1978).

A variety of textural and compositional criteria

* Present address: Department of Geological Sciences, McGill University, Montreal, Quebec, Canada H3A 2A7

Mineralogical Magazine, September 1990, Vol. 54, pp. 367–380

has been cited to distinguish between a xenocrystic and magmatic origin for garnets in granitoid rocks. Well-formed and unzoned garnets are generally inferred to be phenocrysts (e.g. Green and Ringwood, 1968; Harrison, 1988), although original grain shapes may be modified by reaction with magma, particularly in the case of garnets transported to shallow structural levels during emplacement. Distinction of garnet phenocrysts and xenocrysts on textural grounds is hampered by the fact that xenocrysts also tend to be partly resorbed. Consequently, attention has focused on compositional criteria for interpreting the origin of garnet in these rocks.

Whereas the composition of garnet xenocrysts depends solely on the bulk composition and metamorphic grade of the source rock, the composition of garnet phenocrysts records the effects of magma composition as well as various intensive variables (particularly pressure). Of course, primary zoning patterns may be modified by subsequent reaction with magma or other ferromagnesian phases.

Since garnet fractionates Mn more readily than most other common minerals, an increase in the spessartine content of garnet stabilizes this mineral to low pressures (Green, 1977; Miller and Stoddard, 1978, 1981). On the other hand, experimental studies by Green (1977) demonstrate that grossular and spessartine concentrations in near-liquidus magmatic garnet vary antipathetically. Grossular content is controlled by bulk composition, and increases (at the expense of Mn) with depth of crystallization.

Although many garnets interpreted as phenocrysts are spessartine-rich ($X_{Mn} = 0.1$–0.8; e.g. Miller and Stoddard, 1978, 1981), other magmatic garnets are essentially almandine-pyrope solutions (e.g. Fitton, 1972). Moreover, many metamorphic garnets (particularly in low-grade granitic rocks) contain significant non-femic components, and therefore cannot be readily distinguished from their magmatic counterparts simply on compositional grounds.

The possibility of a metamorphic origin must also be addressed for garnetiferous plutons occurring in metamorphic terranes (compare e.g. Chamberlain and Lyons, 1983, and Plank, 1987). In some plutons (notably mafic intrusions), garnet occurs as a coronal phase, particularly in areas of low-strain. The origin of coronal garnet is problematic, since coronas may form during subsolidus cooling (e.g. Sørenson, 1979) or during a metamorphic overprint (Davidson and van Breemen, 1988). Joesten (1986*a*) recently suggested that some coronas traditionally interpreted as subsolidus features may actually have a magmatic origin, but this hypothesis has met with some resistance (see Ashworth, 1986, and Joesten, 1986*b*).

In this study, we report on the occurrence of coronitic and non-coronitic garnets in a metaluminous granitic–charnockitic pluton. This intrusion, the Potato Hill pluton (Fig. 1), is part of a voluminous suite of Grenvillian (*c*. 1050 Ma; U–Pb, zircon; Baadsgaard *et al.*, in prep.) granites emplaced in high-grade, polymetamorphic gneiss of the Grenville Province of southern Labrador and in correlative rocks of the Long Range Inlier (Owen, in press) of western Newfoundland. Textural and compositional criteria indicate a multifarious origin for garnets in the pluton.

Regional geology

The Long Range Inlier (Fig. 1) is the largest basement massif in the northern Appalachians. It consists primarily of (1) an amphibolite- to granulite-facies gneiss complex (Owen and Erdmer, 1989) derived from quartzofeldspathic protoliths at least 1.55 Ga old (Baadsgaard *et al.*, in prep.) and (2) a variety of felsic to mafic plutonic rocks. Most plutons are megacrystic to equigranular, hornblende–biotite granites (*sensu lato*). Two plutons [the Potato Hill pluton (PHP) and the Lake Michel intrusive suite (LMIS)] also contain charnockitic rocks. Garnet is apparently restricted to the PHP.

A regional, medium-grade (amphibolite facies) tectonothermal event (*c*. 970 Ma; U–Pb and Pb–Pb, titanite and apatite; Baadsgaard *et al.*, in prep.) overlapped terminal stages of Grenvillian plutonism, and produced a regional schistosity in many of the plutons and the country rock.

Petrography

The PHP is a small ($65\,km^2$) intrusion. Three distinct granitoid rock types are distinguished: (1) green–brown, coronitic, garnetiferous charnockite; (2) buff to rose, equigranular, garnetiferous hornblende–biotite granite; and (3) dark grey, megacrystic hornblende–biotite ± garnet granite to granodiorite. The modal composition of each unit is illustrated in Fig. 2.

The charnockite is a massive to weakly foliated, green to green–brown rock containing clino- and orthopyroxene and hornblende which have locally developed garnetiferous corona structures. The charnockite is retrograded to mylonitic hornblende–biotite–garnet granite in high-strain zones near the southern margin of the pluton. A small ($c.\,3\,km^2$) satellite pluton of coronitic charnockite occurs 10 km west of the PHP (Fig. 1, inset). Corona structures in both plutons separate pyroxene,

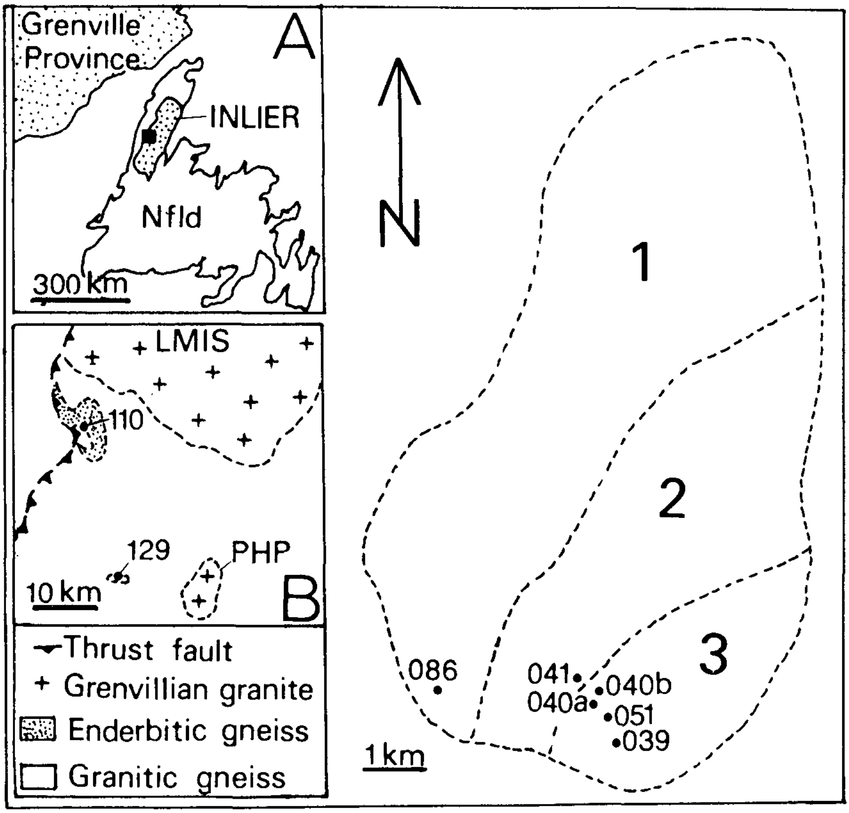

FIG. 1. Geological sketch map of the Potato Hill pluton showing sample locations. 1, megacrystic granite; 2, equigranular granite; 3, charnockite. Insets show (A) the position of the Long Range Inlier relative to the southeastern Grenville Province, and (B) the geology of the west-central part of the inlier (note the location of the charnockitic satellite pluton (sample V087-129) and of coronitic enderbite of the Long Range gneiss complex (sample V086-110)).

ilmenite and primary hornblende from feldspar. The coronas typically consist of inner layers of hornblende and/or quartz, and an outer fringe of fine grained (*c.* 0.2 mm) garnet. Subidiomorphic, olive–green hornblende in the matrix is interpreted as an igneous phase. Clinopyroxene forms xenomorphic to subidiomorphic crystals (to 0.4 mm). The clinopyroxene is subordinate to larger (to 2 mm), subidiomorphic orthopyroxene. Idiomorphic brown biotite (1 mm) is an accessory phase in some samples.

The equigranular granite is a massive, homogeneous rock, but some outcrops exhibit a layered structure outlined by narrow (10 cm wide), mesocratic bands resembling igneous lamination (Fig. 3A). Garnet occurs as (1) irregularly-distributed, xenomorphic to idiomorphic matrix grains or grain aggregates up to 1 cm across (Fig. 3B); (2) smaller, xenomorphic to subidiomorphic crystals concentrated with biotite and hornblende in mesocratic layers; and (3) large (to 4 cm), idiomorphic crystals in diffuse leucocratic segregations (Fig. 3C). Most of the garnets are partly enclosed or veined by hornblende and/or biotite (Fig. 4A). Hornblende and biotite also form mafic clots up to 5 mm in diameter in the matrix of the rock.

The megacrystic granite is a well-foliated, mesocratic (colour index *c.* 15) rock. Foliation is defined by preferentially-oriented K feldspar megacrysts, quartz ribbons, and elongated hornblende-biotite aggregates. Garnet was identified in only one outcrop, where it forms tiny (0.05 to 0.3 mm), xenomorphic to subidiomorphic grains associated with hornblende and biotite (Fig. 4B). Some garnets contain a few quartz oikocrysts. Hornblende occurs as (1) a 'spongy' aggregate with quartz (resembles retrograded pyroxene), and (2) larger (to 1 mm), subidiomorphic crystals. Biotite forms aggregates of small

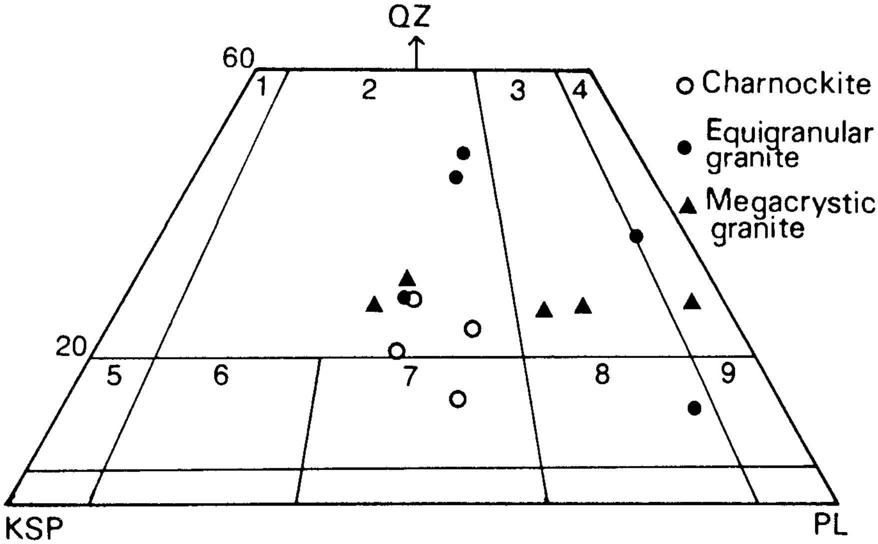

FIG. 2. Modal composition of the Potato Hill pluton. Field boundaries after Streckeisen (1976): 1, alkali feldspar granite; 2, granite; 3, granodiorite; 4, tonalite; 5, quartz alkali feldspar syenite; 6, quartz syenite; 7, quartz monzonite; 8, quartz monzodiorite; 9, quartz diorite.

($\leq$0.3 mm) crystals often associated with hornblende.

K-feldspar throughout the pluton is (locally microperthitic) microcline. Plagioclase is calcic oligoclase to sodic andesine (An_{25-35}). Large (to 0.5 mm), well-formed zircon and apatite are conspicuous accessory phases. Opaque minerals include ilmenite and subordinate magnetite. Traces of epidote and titanite occur locally in the megacrystic and equigranular granites.

Geochemistry

The PHP is an iron-rich intrusion characterized by elevated concentrations of trace elements (e.g. 1200–1700 ppm Zr; 1600–3900 ppm Ba; Owen, in press). Silica varies between 57 and 69 wt.%. The intrusion has an alkali-lime index of *c.* 54. The charnockite and equigranular granite are slightly more ferruginous (bulk $X_{Fe^{2+}}$ [$= Fe^{2+}/(Fe^{2+}+Mg)$ atomic] = 0.91–0.94) than the megacrystic granite (bulk $X_{Fe^{2+}}$ = 0.88–0.90), which rarely contains garnet.

Garnet is apparently absent in coeval Grenvillian plutons in the inlier. Pyroxene-bearing granite of the LMIS is among the most ferruginous of the Grenvillian plutons outside of the PHP. Mean bulk $X_{Fe^{2+}}$ in equigranular and megacrystic charnockite (*sensu lato*) from the LMIS is 0.82 (see data in Owen and Erdmer, in press). Most samples of hornblende-biotite granite in the LMIS and other Grenvillian plutons in the inlier are relatively magnesian (bulk $X_{Fe^{2+}}$ = 0.50 to 0.85). These data point to bulk compositional controls on the formation of garnet (cf. Martignole and Schrijver, 1973), which appears to be restricted to only the most ferruginous granites (i.e. bulk $X_{Fe^{2+}} > 0.9$).

Mineral chemistry

Mineral compositions for all samples except one were determined with a JEOL 733 microprobe equipped with four wavelength-dispersive spectrometers and one energy-dispersive spectrometer, and operated with a beam current of 15kV at 5nA. Data were reduced using ZAF corrections. Count time was 30 s. Sample VO86–110 was analysed with a JEOL JXA-50A microprobe equipped with three wavelength-dispersive spectrometers, operated with a beam current of 15 kV at 22 nA.

As expected from the bulk chemical data, all mafic minerals are ferruginous. Garnet approaches a binary Fe–Ca composition, with subordinate Mn and minor Mg (Table 1). Coronal garnet in unstrained charnockite contains vermicular quartz intergrowths, particularly near its xenomorphic, inner (i.e. corona-side) edge (Fig. 4C). The outer side of the garnet (i.e. where it impinges on matrix feldspar) is idiomorphic. Relatively large (to 1 mm), quartz-free garnets

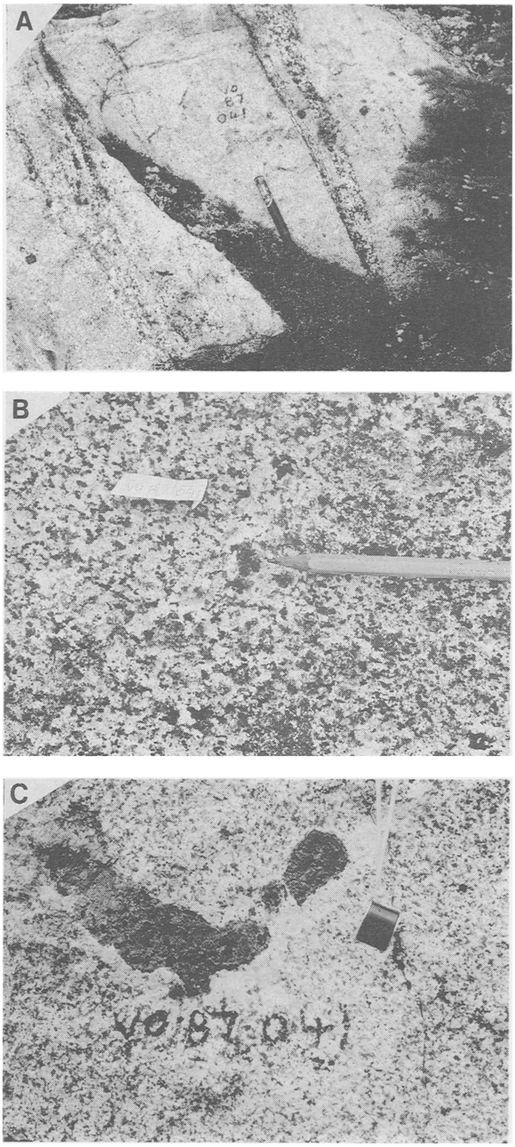

FIG. 3. Field photographs of equigranular granite of the Potato Hill pluton. (A) Mesocratic igneous (?) layers enriched in garnet, hornblende and biotite. (B) garnet in relatively leucocratic granite. (C) large, well formed garnet in diffuse leucocratic segregation.

occur locally in the matrix near corona sites. Garnet in the charnockite contains approximately 70% almandine, 21% grossular, 4% spessartine and 5% pyrope. Garnet in deformed (retrograded) charnockite near the southern margin of the pluton is enriched in spessartine (*c*. 10–12%)

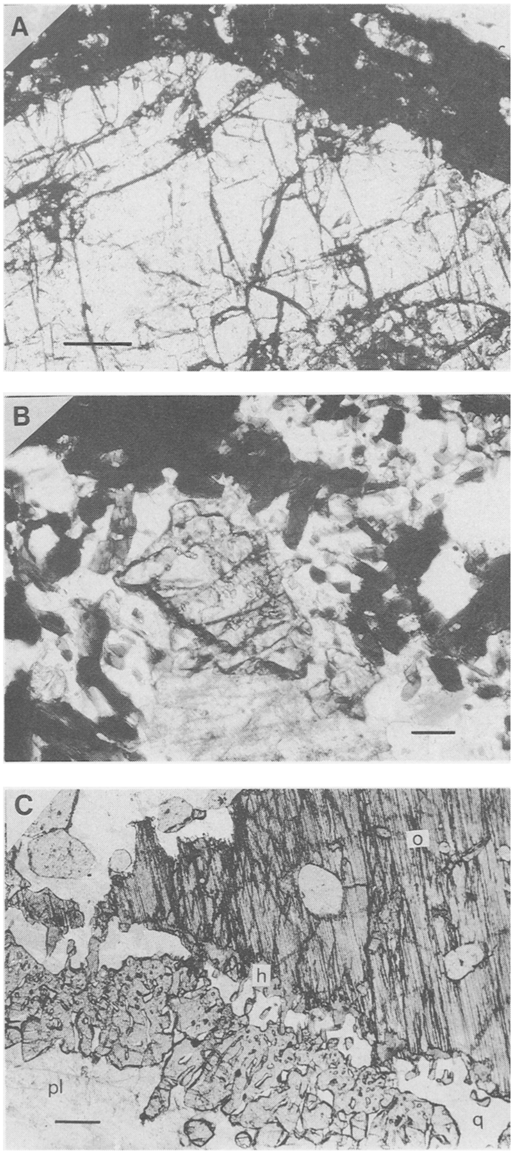

FIG. 4. Photomicrographs of garnets in the Potato Hill pluton. (A) Part of a large (1 cm), idiomorphic garnet in leucocratic, equigranular granite. Note hornblende–biotite mantle. Sample V087-041. Bar = 0.5 mm. (B) Garnets associated with hornblende and biotite in megacrystic granite. Sample V087-086. Bar = 0.1 mm. (C) Coronal garnet in charnockite. Note vermicular quartz intergrowths in garnet. Sample V087-040A. o = orthopyroxene; h = hornblende; q = quartz; pl = plagioclase. Bar = 0.1 mm. All photos taken under plane polarized light.

Table 1 Microprobe analyses of garnet in granitoid rocks of the Potato Hill Pluton

Rock:	Charnockite				Granite			Megacrystic granite
Sample:	(mean of 3)[A]	V087-039-1[B]	V087-039-2[C]	V087-129[D]	V087-041A[E]	V087-041B[F] core	V087-041B[F] rim	V087-086
SiO_2	37.07	37.03	36.88	36.21	37.59	36.85	37.09	36.62
Al_2O_3	20.37	20.75	20.24	20.58	20.31	20.00	20.61	20.67
FeO[G]	32.62	30.77	27.99	32.41	25.87	32.00	29.73	24.22
MnO	1.62	4.47	5.55	1.86	5.70	2.07	5.03	8.75
MgO	1.24	0.85	0.73	0.72	0.70	1.03	0.49	0.39
CaO	7.67	7.43	8.44	7.79	9.89	7.94	7.66	9.07
	100.59	101.30	99.83	99.57	100.06	99.89	100.61	99.72
X_{Mg}	0.048	0.033	0.028	0.028	0.027	0.040	0.019	0.015
X_{Fe}	0.705	0.664	0.612	0.711	0.568	0.694	0.653	0.534
X_{Ca}	0.212	0.205	0.236	0.219	0.278	0.221	0.216	0.256
X_{Mn}	0.035	0.098	0.123	0.041	0.127	0.045	0.112	0.195

Notes:
[A] coronitic garnets in samples V087-040B, 040A1, 051
[B] charnockite near mylonite
[C] mylonitized charnockite
[D] mean coronitic garnet in satellite pluton
[E] matrix garnet in leucocratic granite
[F] garnet in mesocratic layer
[G] total Fe as FeO

and slightly depleted in almandine (*c.* 60–65%) and pyrope (*c.* 3%). Garnet compositions are homogeneous within resolution of the microprobe (i.e. are not zoned), and show little variation between corona types (Table 2).

Garnet in the equigranular granite is relatively enriched in grossular and spessartine, and depleted in almandine, but its composition varies with mode of occurrence. Matrix grains in homogeneous parts of the granite have lower almandine (57%) and higher grossular (28%) and spessartine (13%) contents than garnet in mesocratic layers in the granite. Matrix garnets are not zoned, but garnet in mesocratic layers shows a decrease in Fe and Mg towards the rim, and an increase in Mn. No analytical data are available for large garnets in leucocratic segregations in the granite.

Garnet in megacrystic granite contains the highest concentration of spessartine (20%), and the lowest concentrations of almandine (53%) and pyrope (2%) of any garnets in the pluton. The garnets are not zoned.

It is worthwhile noting that garnet in the PHP is depleted in Mg and enriched in Ca and Mn compared with garnet in paragneiss and orthogneiss of the Long Range gneiss complex (cf. Owen and Erdmer, 1989). Only garnet in Fe-rich, coronitic enderbite (i.e. orthopyroxene-bearing tonalitic gneiss) cropping out 25 km northwest of the PHP (Fig. 1, inset) is compositionally-similar to that in the pluton (cf. Tables 1, 3).

Amphibole forms green, subidiomorphic to xenomorphic, matrix grains in all parts of the pluton. It also is a coronal phase in the charnockite. Both types of amphibole are compositionally similar (Table 2). Classification of the amphibole is sensitive to the recalculation procedure. We have recalculated microprobe analyses of amphiboles to 23 oxygens, and have normalized all cations except Ca, Na and K to 13, after which the ferric iron was estimated by charge balancing. The allocation by this method of alkalis between the *A* and *M*4 structural sites is appropriate for many calcic amphiboles (Robinson *et al.*, 1982). By this procedure, amphibole in all units has significant *A*-site alkalis [$(Na + K)^A$ exceeds 0.5] and an oxidation ratio [$=Fe^{3+}/(Fe^{2+}+Fe^{3+})$] of 0.1–0.2. The composition of the amphibole corresponds to hastingsitic hornblende according to the nomenclature of Leake (1978).

Pyroxene is restricted to the charnockite. Clinopyroxene forms untwinned, xenomorphic grains; in places, it encloses orthopyroxene, and in one sample (VO87–040) clinopyroxene also occurs locally as exsolved blebs within orthopyroxene. The clinopyroxene is ferroaugite to ferrohedenbergite, with X_{Mg} of *c.* 0.25–0.32 (end-member composition *c.* $Wo_{45}En_{19}Fs_{36}$). Some grains show

Table 2 Microprobe analyses of coronal minerals in charnockite of the Potato Hill pluton. "Parent" minerals are underlined. The cpx- and ilm-centered coronas in sample V087-040B share the same plagioclase (i.e., adjacent coronas). The mode of coronal phases is indicated [vol.% of coronal quartz in square brackets].

	opx-centered/V087-051				cpx-centered/V087-040B					ilm-centered/V087-040B			hbl-centered/V087-040A1		
	<u>opx</u>	hbl	gt	pl	cpx <u>core</u>	cpx <u>rim</u>	hbl	gt	pl	gt	hbl	<u>ilm</u>	<u>hbl</u>	gt	pl
SiO_2	47.30	40.44	36.88	59.60	48.64	49.01	40.77	36.52	60.61	36.76	39.52		39.61	36.93	60.86
TiO_2	0.39	0.81	0.20	0.12	0.19	0.11	0.65	0.09		0.07	1.27	50.53	1.78	0.08	
Al_2O_3	0.39	10.23	20.41	25.08	1.17	0.92	10.49	20.35	23.58	20.32	11.29		10.90	20.36	24.28
FeO*	43.25	26.61	33.37	0.29	27.26	21.59	26.68	31.93	0.19	31.54	25.42	45.41	25.23	31.47	0.06
MnO	0.75	0.25	1.25	0.07	0.49	0.42	0.23	1.88		1.91	0.19	0.68	0.18	1.48	
MgO	6.48	4.46	0.92	0.08	5.52	5.61	4.44	1.05		1.02	4.60	0.01	4.43	1.32	
CaO	1.33	11.30	7.33	6.86	16.61	21.10	10.99	7.68	5.55	7.76	11.05	0.06	11.27	7.70	6.37
Na_2O	0.12	1.40		7.68	0.42	0.36	1.24		8.35		1.67		1.65		8.40
K_2O	0.08	1.71		0.24			1.30		0.08		1.33		1.62		0.12
	100.09	97.21	100.36	100.02	100.30	99.12	96.79	99.50	98.32	99.38	96.34	96.69	96.67	99.34	100.09
OB**	3	23	12	8	3	3	23	12	8	12	23	3	23	12	8
Si	0.986	6.466	2.983	2.662	0.977	0.983	6.512	2.976	2.737	2.993	6.334		6.338	2.999	2.709
Al^{iv}	0.014	1.534	0.017	1.321	0.023	0.017	1.488	0.024	1.255	0.007	1.666		1.662	0.001	1.274
Al^{vi}	--	0.394	1.929		0.005	0.005	0.487	1.931		1.943	0.467		0.394	1.948	
Ti	0.006	0.097	0.012	0.004	0.003	0.002	0.078	0.006		0.004	0.153	0.994	0.214	0.005	
Fe	0.754	3.558	2.258	0.011	0.458	0.362	3.564	2.176	0.007	2.148	3.407	0.994	3.376	2.137	0.002
Mn	0.013	0.034	0.086	0.003	0.008	0.007	0.031	0.130		0.132	0.026	0.015	0.024	0.102	
Mg	0.201	1.063	0.111	0.005	0.165	0.168	1.057	0.128		0.124	1.099	0.001	1.056	0.160	
Ca	0.030	1.936	0.635	0.328	0.358	0.454	1.881	0.671	0.269	0.677	1.898	0.002	1.932	0.670	0.304
Na	0.005	0.434		0.665	0.016	0.014	0.384		0.731		0.519		0.512		0.725
K	0.002	0.349		0.014			0.265		0.005		0.272		0.331		0.007
Mode (vol.%)		14	71				39	57		73	17			100	
[vol.% qtz]			[15]					[4]			[10]				
Molar vol.(cm^3)	32.89	~278	117.46	100.30	35.12	35.82	~278	117.48	100.26	117.52	~278	31.69	~278	117.33	100.28
X_{Mg}^{hbl}		0.230					0.229				0.244		0.238		
X_{An}^{pl}				0.326					0.267						0.293
garnet:															
X_{Mg}			0.036					0.041		0.040				0.052	
X_{Fe}			0.731					0.701		0.697				0.696	
X_{Ca}			0.206					0.216		0.220				0.218	
X_{Mn}			0.028					0.042		0.043				0.033	
pyroxene:															
X_{Mg}	0.211				0.265	0.316									
Mol.% Wo	3.0				35.0	44.7									
En	20.5				18.4	18.7									
Fs	~76.5				46.6	36.7									
others***	3.6				9.3	7.7									

Notes:
* total Fe as FeO
** OB = oxygen basis
*** non-quadrilateral components

Table 3 Microprobe analyses of pyroxenes and coronal garnet in enderbitic gneiss (sample V086-110)

	contiguous pair		contiguous pair (corona)			
	cpx	opx	cpx core	cpx rim	gt rim	gt core
SiO_2	48.38	46.95	49.02	49.72	37.49	38.46
TiO_2	0.12	0.08	0.18	0.11		
Al_2O_3	1.04	0.36	0.97	0.96	19.77	20.10
FeO*	26.43	46.97	27.49	25.00	32.30	32.27
MnO	0.68	1.51	0.62	0.49	2.72	2.19
MgO	3.27	3.83	3.49	3.29	0.56	0.62
CaO	19.18	0.93	19.20	18.73	7.49	7.50
Na_2O	0.44	0.02	0.45	0.35		
	99.54	100.65	101.42	98.65	100.33	101.14
garnet:						
X_{Mg}					0.022	0.024
X_{Fe}					0.708	0.714
X_{Ca}					0.210	0.213
X_{Mn}					0.060	0.049
pyroxene:						
X_{Mg}^{Px}	0.180	0.127	0.184	0.190		
Mol.%Wo	41.8	2.2	41.0	40.4		
En	11.1	12.5	11.6	11.3		
Fs	47.1	85.3	47.4	48.3		
others***	8.3	4.5	8.8	4.7		

* total Fe as FeO
** OB = oxygen basis
*** others = non-quadrilateral components

a rimward increase in Ca and X_{Mg} (Table 2). Orthopyroxene forms larger (to 2 mm), twinned, subidiomorphic grains. The orthopyroxene is eulite, with X_{Mg} of about 0.20–0.25 (end-member composition *c.* Wo_3 En_{27} Fs_{75}). Comparison of $X_{Fe^{2+}}$ and $Ca/(Ca+Mg+Fe^{2+})$ indicates a metamorphic composition for the orthopyroxene (Fig. 5). Reintegration of orthopyroxene containing exsolved clinopyroxene blebs increases the Ca content to a concentration more typical of igneous pyroxenes. Both types of orthopyroxene are locally rimmed by quartz–hornblende–garnet coronas.

Origin of non-coronitic garnet

The following observations are pertinent to the interpretation of garnet in the equigranular granite: (1) garnet shows no spatial relationship to gneissic xenoliths, which occur only very locally, and in any case lack garnet; (2) garnet is essentially inclusion-free, and forms large, (sub)idiomorphic crystals occurring in several modes of occurrence; and (3) many of the garnets are rimmed (or criss-crossed) by hornblende or biotite; garnet in leucocratic segregations shows an antipathetic relationship with these minerals.

The spatial association of some garnets with mesocratic layers of presumed igneous origin strongly suggests a magmatic origin. Zoning patterns in these garnets (i.e. increase in Mn/Ca and Fe/Mg towards the rim) are characteristic of continued crystallization under declining *T* and *P* conditions (e.g. as the host magma was emplaced to shallower structural levels; Green, 1977). Since these garnets occur in well-preserved compositional layers, rather than as isolated matrix grains, an alternative interpretation is required. The extensive replacement of garnet by hornblende and biotite in the mesocratic layers suggests subsolidus reaction relations between these phases, which would account for the observed zoning patterns (cf. Schneider, 1975). Lack of zoning in garnets analysed from more leucocratic layers of the granite probably results from less extensive replacement by hornblende and biotite.

Leucocratic segregations enclosing large, idiomorphic garnets are interpreted as reaction haloes within which garnet formed at the expense of hornblende and biotite. Texturally, these segregations resemble leucosomes in migmatite. In this case, the garnets would represent an anhydrous restite phase formed during vapour-absent (dehydration) melting (Thompson, 1982; Waters, 1988) of hornblende–biotite granite. Alternatively, the (hornblende + biotite)-out reaction

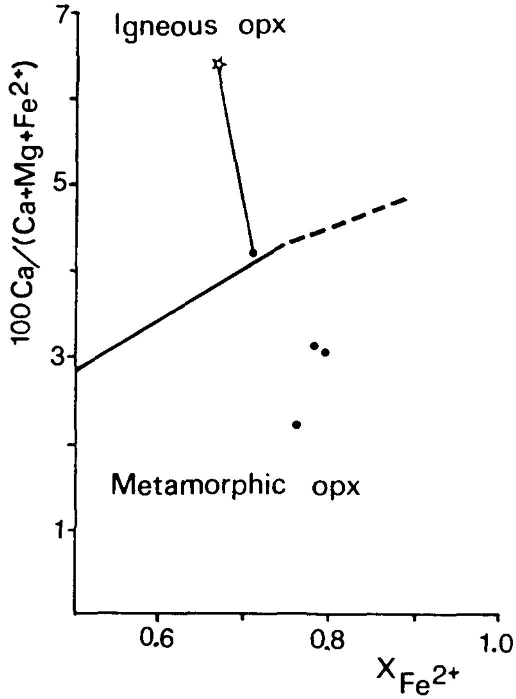

FIG. 5. Plot comparing $Fe^{2+}/(Fe^{2+} + Mg)$ and $Ca/(Ca + Fe^{2+} + Mg)$ in orthopyroxene from two-pyroxene charnockite of the Potato Hill pluton. Line separating compositional fields of igenous and metamorphic pyroxenes is from Rietmeijer (1983). $X_{Fe^{2+}}$ determined by the method of Hamm and Vieten (1971). Tie line connects orthopyroxene containing exsolved clinopyroxene with its reintegrated equivalent (star).

may have occurred in the presence of silicate liquid (i.e. bi + hbl + Liq = gt). Insufficient data are available to clearly distinguish between these two hypotheses, however, in the light of our consideration of other textural occurrences of garnet in the equigranular granite, we prefer the latter interpretation.

The following observations are pertinent to the interpretation of garnet in the northern part of the pluton: (1) the megacrystic granite is pervasively foliated (i.e. contains a well-developed schistosity); (2) garnet forms unzoned, xenomorphic crystals enriched in spessartine ($X_{Mn} = 0.20$); (3) garnet is associated with mafic clots; (4) some garnets contain quartz oikocrysts, and embay nearby amphibole.

As noted earlier, the relatively high Mn content of these garnets does not necessarily imply a magmatic origin, since metamorphic garnets in many low grade granitoid rocks have similar compositions (e.g. Owen, 1988). Texturally and compositionally, garnet in the megacrystic granite is similar to that in the mylonitized charnockite: both form tiny crystals depleted in Mg–Fe and enriched in non-femic components relative to garnet in less highly deformed parts of the pluton. Although a magmatic origin cannot be excluded, all evidence points to a metamorphic origin for garnet in the megacrystic granite. We therefore suggest that these garnets formed (or re-equilibrated) during ductile deformation of the northern part of the pluton. Microstructural evidence suggests that the garnet formed at the expense of hornblende.

Origin of the garnetiferous corona structures

Coronas are disequilibrium features in which both reactant and product phases are preserved. Despite this, the reconstruction of corona-forming reactions is not a trivial task, since these reactions can occur in several stages (e.g. Mall and Sharma, 1988), and can involve the introduction or loss of mobile components. Four principal types of corona structures have been recognized in the charnockite (Marr, 1989):

Type (1) coronas comprise a central core of orthopyroxene surrounded in turn by a narrow (0.1 mm), discontinuous rim of hornblende (in places absent), quartz, and garnet. The coronas are developed adjacent to plagioclase or K-feldspar, but not quartz.

Type (2) coronas are similar to Type (1) coronas, except that it is clinopyroxene (not orthopyroxene) which forms the central core, and is rimmed by hornblende and garnet adjacent to feldspar. A rare variant of types (1) and (2) coronas has a central core of orthopyroxene enclosed by clinopyroxene, which is separated from adjacent plagioclase by quartz and garnet. Clinopyroxene-centred coronas compositionally-similar to those in the charnockite occur in enderbite from the Long Range gneiss complex (Fig. 1, inset; Table 3). As in charnockite of the PHP, coronal garnet in the enderbite contains vermicular quartz intergrowths. These coronas differ, however, in the absence of an intervening hornblende–quartz moat separating garnet from the pyroxene core. Furthermore, orthopyroxene in the gneiss is non-coronitic.

Type (3) coronas consist of a central core of ilmenite armoured by hornblende, in places with an outer necklace of garnet. Either garnet or hornblende may be absent along the interface between ilmenite and feldspar. Ilmenite is generally separated from nearby orthopyroxene by a thin rim of hornblende.

In Type (4) coronas, garnet separates igneous-

Table 4. Balanced mass transfer reactions for pyroxene-centred coronas in charnockite of the Potato Hill pluton. Reactions are constrained by the assumptions of constant volume and constant Al, and are based on the modal, molar volume and microprobe data in Table 2. The cpx-centred corona uses the rim composition of the clinopyroxene.

opx-centered

1.000 opx + 9.268 pl + 0.482 H_2O + [14.003 Fe + 1.559 Ca + 1.203 Si + 0.911 Mg + 0.463 Mn + 0.036K] =

5.821 grt + 6.379 qtz + 0.482 hbl + [5.959 Na]

cpx-centered

1.000 cpx + 15.850 pl + 2.281 H_2O + [24.809 Fe + 4.862 Ca + 3.252 Mg + 1.089 Mn + 0.525 K + 0.223 Ti] =

7.883 grt + 2.854 qtz + 2.281 hbl + [10.724 Na + 6.050 Si]

appearing hornblende from feldspar. These hornblende-centred coronas are relatively rare. As noted earlier, the primary hornblende is similar in composition to the coronal amphibole. Minor contrasts in amphibole compositions between corona types reflect the influence of the 'parent' phase. For example, amphibole in ilmenite-centred coronas is relatively enriched in Ti compared with coronal hornblende armouring orthopyroxene (Table 2). The compositional range of phases in all coronal types is nonetheless remarkably small both within and between samples.

Not all charnockite samples are coronitic. Since all samples were taken in a small area (Fig. 1), intensive variables such as P and T are expected to have been nearly constant. Furthermore, the bulk composition of coronitic and non-coronitic charnockite is nearly indistinguishable, so local variations in major element geochemistry probably did not control the development of the coronas. Rather, factors which may vary substantially on a domainal scale (e.g. fluid compositions and the chemical potential of mobile, reactant elements) likely played a role in controlling the formation of coronas in the charnockite.

Corona-forming equilibria. Corona-forming reactions have been modelled from microprobe data for coronas of known modal composition (Table 2). Modes determined from enlarged photomicrographs were converted to molar proportions using molar volumes calculated from endmember values for the solid solution phases (the molar volume of hornblende was assumed to be 278 cm^3, and of quartz to be 22.688 cm^3). Since the proportions of the product phases are known, the reaction coefficients of the product assemblage may be determined if the coefficient of one phase is calculated. Setting to unity the coefficient of one of the two reactant phases reduces the total number of unknown coefficients to two: one reactant and one product. A unique solution for both coefficients may be determined by holding two variables constant (e.g. two 'immobile' elements, or by assuming constant volume and the constancy of one element). Al and Ti are commonly considered to be relatively immobile in metamorphic reactions; however, Ti is virtually restricted to only two phases (ilmenite and hornblende), so reactions reported here are based on the constancy of both volume and Al. Reaction coefficients were calculated from the simultaneous solution (using matrix algebra: Cramer's Rule) of constant volume and Al expressions for each corona type. This method was successful only for the pyroxene-centred coronas (Table 4); negative coefficients were determined for known reactant and/or product phases in the other corona types. Other constraints applied to the hornblende- and ilmenite-centred coronas (e.g. constant volume and Ti; constant Ti and Al; constant Mg and Fe) were also unsuccessful in this regard. Consequently, ionic communication between these latter coronas and the pyroxene-centred coronas may only be evaluated qualitatively.

As shown by the balanced reactions (Table 4), the pyroxene-centred coronas require a large influx of Fe and smaller amounts of Ca, Mg and Mn. It is unlikely that Fe was provided by the breakdown of igneous-appearing hornblende, since the amphibole has a smaller Fe/Mg ratio (3.2) than its breakdown product (Fe/Mg in garnet = 13.4). Neither are the ilmenite-centred coronas a likely reservoir of Fe, since the oxide breaks down to Fe-rich, Ti-poor phases (garnet, hornblende) so that Ti rather than Fe would be in excess. It is noteworthy that non-coronitic, intergranular ilmenite grains occur locally in the charnockite. These may have formed as excess Ti from the ilmenite-centred coronas was stabilized by migrant Fe, which also contributed to the formation of the various corona types.

The available data suggest that the flux of Fe controlled corona growth in the charnockite. The source of the Fe is not known, although its mobility must be large relative to the scale of the corona structures. All corona types generated excess Na (originating in feldspar), so the system is interpreted to have been open to alkalis. Presumably the apparent influx of Ca, Mg and Mn to the pyroxene-centred coronas is an artifact, at least in part, of the constraints placed on the reactions. This is particularly true for Ca, since the Si/Al ratio of plagioclase varies with anorthite content.

P–T conditions of corona formation. The charnockite contains a plethora of *P*- and *T*-sensitive assemblages; however, many of the pertinent phases occur in corona structures and are therefore metastable.

Potentially, the pressure at which the coronas formed may be estimated from the garnet–pyroxene–plagioclase–quartz geobarometer. Using a quaternary garnet solution model (Hodges and Royden, 1984) an ideal, two-site solution model for orthopyroxene (Wood and Banno, 1973) and Newton's (1983) expression for the activity of anorthite in plagioclase, thermodynamic calibrations of this barometer presented by Newton and Perkins (1982) and Perkins and Chipera (1985; Mg- and Fe-reactions) yield pressures of 7.0, 5.9 and 9.1 kbar, respectively, for a model temperature of 750 °C. These pressures overlap the 5–8 kbar range determined for early, granulite-facies metamorphism of the Long Range gneiss complex (Owen and Erdmer, 1989); however, the local presence of high-grade xenoliths clearly demonstrates that the PHP postdates regional granulite facies metamorphism. The structural depth of formation of the coronas remains poorly constrained, however, because (1) coronitic garnet-orthopyroxene–plagioclase–quartz constitutes a disequilibrium assemblage, and (2) the garnets have a low Mg/Mn ratio (*c*. 1.4), which further renders application of this barometer suspect.

Since both ortho- and clinopyroxenes of probable igneous origin core corona structures, two-pyroxene thermometry should constrain the upper temperature limit of formation of the coronas. Of the numerous calibrations available, Sen (1985) concluded from experimental data on spinel peridotites that Well's (1977) method provides relatively reliable temperatures. Application of Well's calibration to pairs of pyroxene grains (including exsolved clinopyroxene in eulite) from the charnockite yields temperatures of about 750–775 °C (Table 5). These temperatures are at least 150 °C lower than anticipated for igneous pyroxenes crystallized from Fe-rich charnockitic rocks (cf. Rietmeijer, 1979), and are more indicative of subsolidus, granulite-facies conditions. The two-pyroxene temperatures are interpreted to record the conditions at which volume diffusion processes involving pyroxenes were quenched. This may account for the 'metamorphic' composition of the orthopyroxene according to Rietmeijer's (1983) criteria (Fig. 5). Continued down-temperature re-equilibration of pyroxene compositions would be facilitated by slow subsolidus cooling, e.g. as would be the case if the ambient temperature of the gneissic country rock was fairly high at the time of emplacement. Slow cooling of the pluton would also promote the formation of subsolidus coronas.

Where in mutual contact, coronal hornblende and garnet likely preserve local equilibrium compositions, and provide a more direct means of estimating *T* for these coronas. The garnet-hornblende geothermometer (Graham and Powell, 1984) yields temperatures ranging from 630 to 660 °C for sample VO87–040A.

Discussion

No single process explains all of the contrasting textural and compositional features characterizing garnets in the PHP. Of the four principal competing models for garnet in granitoid rocks—xenocrystal, magmatic, subsolidus cooling, or metamorphic—the first may be disregarded owing to the compositional dissimilarity of garnet in the PHP and the gneissic country rock throughout the inlier.

Garnetiferous coronas similar to those in the PHP occur in the Bengal area of eastern India. Manna and Sen (1974) proposed a subsolidus-cooling model for these coronas based on a comparison of Mg–Fe distribution coefficients (*Kd*) of coexisting mafic phases in garnetiferous and non-garnetiferous lithologies. Their interpretation has recently been challenged by Bhattacharyya and Mukherjee (1987), who pointed out the role of bulk compositions in influencing *Kd*'s in these rocks. Bhattacharyya and Mukherjee rejected the subsolidus-cooling model in favour of a metamorphic origin for the coronas, which

Table 5. Mineral chemistry and temperature estimates of contiguous ortho- and clinopyroxene pairs from charnockite of the Potato Hill pluton (samples V087-040A,B)

	V087-040A								V087-040B	
					Pair 3					
	Pair 1		Pair 2		opx	exsolved		reintegrated	Pair 1	
	opx	cpx	opx	cpx	host	cpx	sd*	comp.**	opx	cpx
SiO_2	48.02	49.48	47.81	49.22	48.20	50.32	0.34	48.26	48.41	49.80
TiO_2	0.17	0.24	0.15	0.16	0.11	0.13	0.04	0.11	0.10	0.15
Al_2O_3	0.32	1.44	0.40	1.25	0.49	0.91	0.11	0.50	0.32	1.13
Cr_2O_3	0.08	0.07	0.06	0.08	0.11	0.08	0.02	0.11	0.11	0.06
FeO	45.05	23.66	44.75	23.57	41.80	21.23	0.46	41.19	44.15	22.04
MnO	1.60	0.74	1.57	0.77	0.75	0.33	0.05	0.74	0.90	0.41
MgO	5.00	4.49	4.92	4.27	7.06	6.03	0.14	7.03	6.25	5.43
CaO	1.05	20.97	1.05	20.58	1.45	21.48	0.34	2.05	0.86	21.03
Na_2O	0.05	0.41	0.03	0.43	0.08	0.38	0.05	0.09	0.02	0.47
	101.34	101.50	100.74	100.33	100.05	100.89		100.08	101.12	100.52
Endmember Comp.:										
Mol.% Wo	2.4	43.6	2.5	44.0	3.3	45.2		4.7	2.0	44.6
En	16.1	15.1	16.0	14.3	22.4	19.2		22.2	19.8	17.8
Fs	81.5	41.3	81.6	41.7	74.3	35.6		73.1	78.3	37.6
others***	4.2	9.6	4.2	8.5	3.2	6.5		3.2	2.8	8.0
T°C (Wells,1977)	767		757		769				775	

* sd = one standard deviation (n = 13)

** exsolved cpx blebs occupy 3 vol. % of opx host

***others = non-quadrilateral components

they proposed to have formed by prograde dehydration reactions. In the case of the PHP, however, a metamorphic-overprint model is untenable since corona structures were destroyed, not created, by subsequent (late Grenvillian) metamorphism. We therefore conclude that the coronas formed during subsolidus cooling following emplacement and consolidation of the pluton. Although age constraints are lacking, compositionally-similar coronas in Fe-rich enderbite of the Long Range gneiss complex (sample VO86–110) are interpreted to have formed during cooling after early (i.e. pre-PHP), granulite-facies metamorphism, or following the regional emplacement of the Grenvillian granitoid plutons.

Coronas comprise a plethora of phases, and typically form as a result of coupled reactions. Corona reactions on the scale of a hand sample were largely closed to most components except Fe and Na. This may explain the local absence of corona structures in the charnockite. If our model is correct, coronas would not develop without an influx of Fe. We therefore conclude that diffusion-controlled corona growth was dominated by the mobility of Fe relative to other components, and that the phenomenological diffusion coefficients (Brady, 1975) for Fe were large.

Compared with the low-strain protolith, garnet in the recrystallized charnockite is fine grained, and is enriched in Ca and Mn, and depleted in Fe and Mg. Fine-grained garnet occurring locally in megacrystic granite has the lowest Fe–Mg and highest non-femic composition of any garnet in the pluton. By analogy with garnet in the deformed charnockite, this garnet is interpreted to have formed (or re-equilibrated) during the same tectonothermal event.

Garnets in the equigranular granite are interpreted as phenocrysts since they occur as large, well formed crystals that are in places associated with structures of possible igneous origin. However, these garnets have higher Ca and lower Mn than magmatic garnets in many other plutons (cf. Manning, 1983; Allan and Clarke, 1981; Vennum and Meyer, 1979), indicating either unusual crystallization conditions or the unusual bulk composition of this pluton.

The composition of these garnets has implications for the silicic magma from which they are inferred to have crystallized. Green (1977) demonstrated that the extent to which garnet fractionates Mg and Fe relative to silicic magma varies with T. Above 950°C, Mg/(Mg+Fe) is greater in garnet than the coexisting magma; the converse is true below this temperature. As noted by Green (1977), this has important implications for the Mg/Fe ratio of residual liquids during cooling, since the tendency for progressive Fe-enrichment will be somewhat diminished if garnet continues to crystallize below 950°C. The extent to which garnet controlled the chemical evolution of the PHP is not known since relatively primitive, comagmatic rocks have not been identified. Furthermore, Mg/(Mg+Fe) is similar in both the granite (bulk X_{Mg} = 0.07) and garnet from the same sample [Mg/(Mg+Fe) = 0.05], so that no inference can be made concerning the temperature at which garnet crystallized.

Green and Ringwood (1968) demonstrated that almandine-rich garnets with a high Ca/Mn ratio crystallize from silicic calc-alkaline liquids at elevated pressures (> 9 kbar). The elevated Ca/Mn ratio of garnet in the equigranular granite provides evidence for crystallization at considerable depth (probably exceeding 25 km). Their moderate spessartine content, however, would have stabilized these garnets to much shallower structural levels during emplacement.

Conclusions

Almandine–grossular-rich garnets in the Potato Hill pluton are interpreted on textural and compositional grounds to have formed by both magmatic and subsolidus processes. Magmatic garnets are enriched in Ca, and form large, well-developed crystals that are associated with various igneous(?) features (compositional layering; leucocratic reaction haloes). Metamorphic garnets form tiny crystals depleted in Mg and Fe, and enriched in non-femic components; they are restricted to deformed parts of the pluton. Coronal garnet is restricted to charnockitic rocks. The coronas are inferred to have formed during subsolidus cooling of the pluton prior to late Grenvillian deformation, and formed by reaction of pyroxenes, ilmenite and hornblende with feldspar. Coronal reaction mechanisms involved ionic diffusion between corona sites in a system largely closed to all analysed components except Na and Fe. The flux of the latter component apparently controlled corona formation in the charnockite.

Acknowledgements

Fieldwork was funded by Department of Supply and Services Canada contract 34SZ–23233–7–007. Analytical work was supported by Natural Sciences and Engineering Research Council of Canada grant #OGP0037241. Thanks are extended to an anonymous referee for advice on balancing corona reactions.

References

Allan, B. D. and Clarke, D. B. (1981) Occurrence and origin of garnets in the South Mountain batholith, Nova Scotia. *Can. Mineral.* **19,** 19–24.

Ashworth, J. R. (1986) The role of magmatic reaction, diffusion, and annealing in the evolution of coronitic microstructure in troctolitic gabbro from Risor, Norway: a discussion. *Mineral. Mag.* **50,** 469–73.

Baadsgaard, H., Erdmer, P. and Owen, J. V. (in prep.) U–Pb geochronology of the Long Range Inlier, Newfoundland. (submitted to *Geol. Soc. Amer. Bull.*)

Bhattacharyya, P. K. and Mukherjee, S. (1987) Granulites in and around the Bengal anorthosite, eastern India: genesis of coronal garnet, and evolution of the granulite-anorthosite complex. *Geol. Mag.* **124,** 21–32.

Brady, J. B. (1975) Reference frames and diffusion coefficients. *Amer. J. Sci.* **275,** 954–83.

Cawthorn, R. G. and Brown, P. A. (1976) A model for the formation and crystallization of corundum-normative calc-alkaline magmas through amphibole fractionation. *J. Geol.* **84,** 467–76.

——— (1978) A model for the formation and crystallization of corundum-normative calc-alkaline magmas through amphibole fraction: a reply. Ibid. **86,** 272–5.

Chamberlain, C. P. and Lyons, J. B. (1983) Pressure, temperature and metamorphic zonation studies of pelitic schists in the Merrimack Synclinorium, south-central New Hampshire. *Amer. Mineral.* **68,** 530–40.

Davidson, A. and van Breeman, O. (1988) Baddeleyite–zircon relationships in coronitic metagabbro, Grenville Province, Ontario: implications for geochronology. *Contrib. Mineral. Petrol.* **100,** 291–9.

Fitton, J. G. (1972) The genetic significance of almandine-pyrope phenocrysts in the calc-alkaline Borrowdale Volcanic Group, northern England. Ibid. **36,** 231–48.

Graham, C. M. and Powell, R. (1984) A garnet–hornblende geothermometer: calibration, testing, and application to the Pelona Schist, southern California. *J. Metamorphic Geol.* **2,** 13–31.

Green, T. H. (1977) Garnet in silicic liquids and its possible use as a *P–T* indicator. *Contrib. Mineral. Petrol.* **65,** 59–67.

—— and Ringwood, A. E. (1968) Origin of garnet phenocrysts in calc-alkaline rocks. Ibid. **18,** 163–74.

Hamm, H. M. and Vieten, K. (1971) Zur Berechnung der Kristallchemischen Formel und des Fe^{3+}-Gehaltes von Klinopyroxenen aus Elektronen-strahl-Microanalysen. *Neues Jahrb. Mineral. Mh.*, 310–5.

Harrison, T. N. (1988) Magmatic garnets in the Cairngorm granite, Scotland. *Mineral. Mag.* **52,** 659–67.

Hodges, K. V. and Royden, L. (1984) Geological thermobarometry of retrograded metamorphic rocks: an indication of the uplife trajectory of a portion of the northern Scandinavian Caledonides. *J. Geophys. Res.* **89,** 7077–90.

Joesten, R. (1986*a*) The role of magmatic reaction, diffusion and annealing in the evolution of coronitic microstructure in troctolitic gabbro from Risor, Norway. *Mineral. Mag.* **50,** 441–467.

—— (1986*b*) The role of magmatic reaction, diffusion and annealing in the evolution of coronitic microstructure in troctolitic gabbro from Risor, Norway: reply. Ibid. **50,** 474–9.

Kontak, D. J. and Corey, M. (1988) Metasomatic origin of spessartine-rich garnet in the South Mountain batholith, Nova Scotia. *Can. Mineral.* **26,** 315–34.

Leake, B. E. (1978) Nomenclature of amphiboles. *Mineral. Mag.* **42,** 533–63.

Mall, A. P. and Sharma, R. S. (1988) Coronas in olivine metagabbros from the Proterozoic Chotanagpur terrain at Mathurapur, Bihar, India. *Lithos*, **21**, 291–300.

Manna, S. S. and Sen, S. K. (1974) Origin of garnet in the basic granulites around Saltora, W. Bengal, India. *Contrib. Mineral. Petrol.* **44**, 195–218.

Manning, D. A. C. (1983) Chemical variation in garnets from aplites and pegmatites, peninsular Thailand. *Mineral. Mag.* **47**, 353–8.

Marr, R. A. (1989) *Petrography of a Grenvillian, coronitic charnockite, western Newfoundland.* Unpubl. Honours thesis, Saint Mary's University, 41 pp.

Martignole, J. and Schrijver, K. (1973) Effect of rock composition on appearance of garnet in anorthosite–charnockite suites. *Can. J. Earth Sci.* **10**, 1132–9.

Miller, C. F. and Stoddard, E. F. (1978) Origin of garnet in granitic rocks: an example of the role of Mn from the Old Woman-Piute Range, California. *Geol. Assoc. Amer. Abs. with Prog.* **10**, 456.

—— —— (1981) The role of manganese in the paragenesis of magmatic garnet: an example from the Old Woman Piute range, California. *J. Geol.* **89**, 233–46.

Newton, R. C. (1983) Geobarometry of high-grade metamorphic rocks. *Amer. J. Sci.* **283A**, 1–28.

—— and Perkins, D. (1982) Thermodynamic calibration of geobarometers based on the assemblage garnet–plagioclase–orthopyroxene(–clinopyroxene)–quartz. *Amer. Mineral.* **67**, 203–22.

Owen, J. V. (1988) Geochemical changes accompanying the mylonitization of diverse rock types from the Grenville Front zone, eastern Labrador. *Can. J. Earth. Sci.* **25**, 1472–84.

—— (in press) Geology of the Long Range Inlier, Newfoundland. *Geol. Surv. Canada Bull.* 395.

—— and Erdmer, P. (1989) Metamorphic geology and regional geothermobarometry of a Grenvillian massif: the Long Range Inlier, Newfoundland. *Precambrian Res.* **43**, 79–100.

—— —— (in press) Middle Proterozoic geology of the Long Range Inlier, Newfoundland: regional significance and tectonic implications. In *Mid-Proterozoic Geology of the Southern Margin of Proto-Laurentia-Baltica* (Gower, C. F., Rivers, T. and Ryan, A. B., eds.) Geol. Assoc. Canada, Special Volume.

Perkins, D. and Chipera, S. J. (1985) Garnet-orthopyroxene-plagioclase-quartz barometry: refinement and application to the English River sub-province and the Minnesota River valley. *Contrib. Mineral. Petrol.* **89**, 69–80.

Plank, T. (1987) Magmatic garnets from the Cardigan pluton and the Acadian thermal event in southwest New Hampshire. *Amer. Mineral.* **72**, 681–8.

Rietmeijer, F. J. M. (1979) Pyroxenes from iron-rich igneous rocks in Rogaland, SW. Norway. *Geol. Ultraiectina*, **21**, 341 pp.

Rietmeijer, F. J. M. (1983) Chemical distinction between igneous and metamorphic orthopyroxenes especially those coexisting with Ca-rich clinopyroxenes: a re-evaluation. *Mineral. Mag.* **47**, 143–51.

Robinson, P., Spear, F. S., Schumacker, J. C., Laird, J., Klein, C., Evans, B. W. and Doolan, B. L. (1982) Phase relations of metamorphic amphiboles: natural occurrence and theory. In *Amphiboles: Petrology and experimental phase relations* (Veblen, D. R. and Ribbe, P. H., eds.) Mineral. Soc. Amer. *Reviews in Mineralogy*, **9B**, 1–227.

Schneider, G. (1975) Experimental replacement of garnet by biotite. *Neues Jahrb. Mineral. Mh.*, 1–10.

Sen, G. (1985) Experimental determination of pyroxene compositions in the system $CaO–MgO–Al_2O_3–SiO_2$ at 900–1200° using Pb and H_2O fluxes. *Amer. Mineral.* **70**, 678–95.

Sørensen, K. (1979) Are coronas cooling products? *Rapp. Grønlands geol. Unders.* **89**, 113–4.

Stone, M. (1988) The significance of almandine garnets in the Lundy and Dartmoor granites. *Mineral. Mag.* **52**, 651–8.

Streckeisen, A. (1976) To each plutonic rock its proper name. *Earth Sci. Rev.* **13**, 1–33.

Thompson, A. B. (1982) Dehydration melting of pelitic rocks and the generation of H_2O-undersaturated granitic liquids. *Amer. J. Sci.* **282**, 1567–95.

Vennum, W. R. and Meyer, C. E. (1979) Plutonic garnets from the Werner batholith, Lassiter Coast, Antarctic Peninsula. *Amer. Mineral.* **64**, 268–73.

Waters, D. J. (1988) Partial melting and the formation of granulite facies assemblages in Namaqualand, South Africa. *J. Metamorphic Geol.* **6**, 387–404.

Wells, P. R. A. (1977) Pyroxene thermometry in simple and complex systems. *Contrib. Mineral. Petrol.* **62**, 129–39.

Wood, B. J. and Banno, S. (1973) Garnet–orthopyroxene and orthopyroxene–clinopyroxene in simple and complex systems. Ibid. **42**, 109–24.

[*Manuscript received 12 June 1989; revised 7 November 1989*]